



HAL
open science

Structural brain connectivity in children after neonatal stroke: A whole-brain fixel-based analysis

Pablo Pretzel, Thijs Dhollander, Stéphane Chabrier, Mariam Al-Harrach,
Lucie Hertz-Pannier, Mickael Dinomais, Samuel Groeschel

► **To cite this version:**

Pablo Pretzel, Thijs Dhollander, Stéphane Chabrier, Mariam Al-Harrach, Lucie Hertz-Pannier, et al..
Structural brain connectivity in children after neonatal stroke: A whole-brain fixel-based analysis.
Neuroimage-Clinical, 2022, 34, pp.103035. 10.1016/j.nicl.2022.103035 . hal-03689773

HAL Id: hal-03689773

<https://hal.science/hal-03689773>

Submitted on 23 Jan 2023

HAL is a multi-disciplinary open access archive for the deposit and dissemination of scientific research documents, whether they are published or not. The documents may come from teaching and research institutions in France or abroad, or from public or private research centers.

L'archive ouverte pluridisciplinaire **HAL**, est destinée au dépôt et à la diffusion de documents scientifiques de niveau recherche, publiés ou non, émanant des établissements d'enseignement et de recherche français ou étrangers, des laboratoires publics ou privés.



Structural brain connectivity in children after neonatal stroke: A whole-brain fixel-based analysis

Pablo Pretzel^{a,*}, Thijs Dhollander^b, Stéphane Chabrier^c, Mariam Al-Harrach^d, Lucie Hertz-Pannier^e, Mickael Dinomais^f, Samuel Groeschel^a

^a Department of Child Neurology, Paediatric Neuroimaging, University Hospital, Tübingen, Germany

^b Developmental Imaging, Murdoch Children's Research Institute, Melbourne, Australia

^c INSERM U 1059 Sainbiose, Univ Saint-Étienne, Saint-Étienne, France

^d Univ Rennes, INSERM, LTSI – UMR 1099, F-35000 Rennes, France

^e UNIACT/Neurospin/JOLIOT/DRF/CEA-Saclay, and U1141 NeuroDiderot/Inserm, CEA, Paris University, France

^f Department of Physical and Rehabilitation Medicine, University Hospital, CHU Angers, France

ARTICLE INFO

Keywords:

Neonatal arterial ischemic stroke
Fixel-based whole-brain analysis
Interhemispheric white matter tracts
Manual dexterity
Long-term network injury

ABSTRACT

Introduction: Neonatal arterial ischemic stroke (NAIS) has been shown to affect white matter (WM) microstructure beyond the lesion. Here, we employed fixel-based analysis, a technique which allows to model and interpret WM alterations in complex arrangements such as crossing fibers, to further characterize the long-term effects of NAIS on the entire WM outside the primary infarct area.

Materials and methods: 32 children (mean age 7.3 years (SD 0.4), 19 male) with middle cerebral artery NAIS (18 left hemisphere, 14 right hemisphere) and 31 healthy controls (mean age 7.7 years (SD 0.6), 16 male) underwent diffusion MRI scans and clinical examination for manual dexterity. Microstructural and macrostructural properties of the WM were investigated in a fixel-based whole-brain analysis, which allows to detect fiber-specific effects. Additionally, tract-averaged fixel metrics in interhemispheric tracts, and their correlation with manual dexterity, were examined.

Results: Significantly reduced microstructural properties were identified, located within the parietal and temporal WM of the affected hemisphere, as well as within their interhemispheric connecting tracts. Tract-averaged fixel metrics showed moderate, significant correlation with manual dexterity of the affected hand. No increased fixel metrics or contralateral alterations were observed.

Discussion: Our results show that NAIS leads to long-term alterations in WM microstructure distant from the lesion site, both within the parietal and temporal lobes as well as in their interhemispheric connections. The functional significance of these findings is demonstrated by the correlations with manual dexterity. The localization of alterations in structures highly connected to the lesioned areas shift our perception of NAIS from a focal towards a developmental network injury.

1. Introduction

Neonatal Arterial Ischemic Stroke (NAIS) is defined as a cerebral arterial ischemic insult symptomatic within the first 4 weeks of life (Raju et al., 2007). With an estimated prevalence of 1 in 3000 births at term, it is the most common type of perinatal stroke (Dunbar et al., 2020), and

often leaves affected children with severe and lifelong disabilities (Kirton and deVeber, 2013; Fluss et al., 2019).

The extent of the neurological impairments after NAIS varies drastically and can be explained only partly by lesion volume and localization (Lee et al., 2005; Dinomais et al., 2016). Instead, as further elaborated below, numerous imaging studies have provided evidence

Abbreviations: BBT, Box-and-blocks test; CC, Corpus Callosum; FBA, Fixel-based analysis; FC, Fiber cross-section; FD, Fiber density; FDC, Fiber density and cross-section; FOD, Fiber orientation distribution; GM, Grey matter; HC, Healthy controls; LLP, Left-lesioned patients; MCA, Middle cerebral artery; NAIS, Neonatal arterial ischemic stroke; PC, Parietal cortex; PMC, Premotor cortex; RLP, Right-lesioned patients; SMA, Supplementary motor area; TIV, Total intracranial volume; WM, White matter.

* Corresponding author at: Universitäts-Kinderklinik Tübingen, Hoppe-Seyler-Straße 1, 72076 Tübingen, Germany.

E-mail address: pablo.pretzel@med.uni-tuebingen.de (P. Pretzel).

<https://doi.org/10.1016/j.nicl.2022.103035>

Received 9 January 2022; Received in revised form 16 April 2022; Accepted 4 May 2022

Available online 7 May 2022

2213-1582/© 2022 The Authors. Published by Elsevier Inc. This is an open access article under the CC BY-NC-ND license (<http://creativecommons.org/licenses/by-nc-nd/4.0/>).

that NAIS has additional, disseminated effects on brain tissue distant from the primary lesion site. This suggests the understanding of NAIS as a complex network injury, which affects structure throughout the entire brain.

Fixel-based analysis (FBA), a recently introduced method to study WM microstructural and macrostructural properties using diffusion MRI (Raffelt et al., 2015; Raffelt et al., 2017; Dhollander et al., 2021a), allows to expand the understanding of these disseminated effects of NAIS on WM. It enables a whole-brain characterization of alterations in WM structural connectivity without being limited to predefined regions of interest. At the same time, FBA metrics are fiber-specific (a “fixel” refers to an individual fiber population within a voxel), particularly also in the presence of crossing fibers. This is a marked advantage over popular voxel-averaged approaches such as Diffusion Tensor Imaging (DTI), which lack interpretability in the presence of complex fiber arrangements (Jones et al., 2013; Mito et al., 2018). FBA is implemented in the MRtrix software package (Tourneris et al., 2019), and has increasingly been used over recent years (Dhollander et al., 2021a).

In FBA, each fixel is typically assigned quantitative metrics for Fiber Density (FD), Fiber Cross-Section (FC) and Fiber Density and Cross-Section (FDC; D. A. Raffelt et al., 2017). These metrics quantify microstructural changes due to a local loss of intra-axonal volume (FD), macrostructural changes across the diameter (i.e. cross-section) of a fiber bundle (FC), as well as the combination of both micro- and macrostructural alterations (FDC). A detailed discussion of these metrics and their interpretation in various biological example scenarios can be found in Dhollander et al. (2021a).

In the present study, we set out to leverage the advantages of FBA to examine the long-term effects of NAIS on the WM microstructure in a cohort of affected children at the age of 7 years. Previous research on this cohort already provided evidence of alterations in individual WM regions, such as alterations in metrics derived from the diffusion tensor model in the ipsilesional corticospinal tract at the level of the internal capsule and the centrum semiovale (Dinomais et al., 2015), and WM volume reductions in the ipsilesional internal capsule and the body of the corpus callosum (CC) (Dinomais et al., 2016). Recent studies on this cohort notably suggested additional involvement of the contralesional hemisphere after neonatal stroke, such as reduced gyrfication, cortical thickness, surface area and volume primarily in the occipital lobe (Al Harrach et al., 2019), as well as altered connectivity in the contralesional hemisphere as measured by streamline counts (Al Harrach et al., 2021). Contralesional alterations of graph theory metrics were also found in a different cohort of 53 children after arterial or venous unilateral perinatal stroke (Craig et al., 2020), and in a cohort of 104 adults after ischemic stroke, FBA revealed both ipsi- and contralesional alterations of fixel metrics (Natalia et al., 2020). Taken together, these prior studies further emphasize that long-term effects of NAIS should be examined globally. By using FBA, we are able to perform such a global investigation of the effect of NAIS on the WM microstructure in a fiber-specific manner, therefore complementing and improving on the findings of these prior studies.

In our previous works on this cohort, in addition to the aforementioned structural alterations in the contralesional hemisphere, we also found evidence for involvement of interhemispheric connections in the corpus callosum (CC) (Groeschel et al., 2017). Here, a reduction of the area of the CC taken up by streamlines connecting the primary motor cortices was found. Furthermore, the reduction in motor CC area was correlated with dexterity in both the affected and non-affected hand, indicating an impaired interplay between hemispheres after NAIS with functional relevance. Without differentiating for individual parts of the CC, prior studies had already shown DTI metric reductions in the CC in a cohort of 19 children immediately in the days following focal ischemia and other lesions (Righini et al., 2010) as well as 3 months after perinatal arterial ischemic stroke in 16 patients (van der Aa et al., 2013).

In order to expand on these findings by utilizing the advantages provided by FBA, we aimed to further characterize the effect on NAIS on

the interhemispheric connections by analyzing mean fixel values across individual interhemispheric fiber tracts from the sensorimotor network. Furthermore, we specifically aimed to assess the functional relevance of our findings for hand motor performance of our subjects. To this end, we correlated manual dexterity with tract-averaged fixel metrics of those tracts that exhibited significantly reduced mean FDC. An association with manual dexterity in tracts that already present significant differences in mean FDC between groups would serve as an indicator for these structural differences explaining the observed functional differences in manual dexterity between groups.

Our aim in this work was to provide a comprehensive, whole-brain analysis of the long-term effects of NAIS on WM networks beyond the lesion site. In our analyses, we hypothesized to find reduced fixel metrics as an expression of WM impairment caused by the focal ischemic lesion, possibly accompanied by increased metrics due to compensatory processes (Al Harrach et al., 2019).

2. Materials and methods

2.1. Participants

All patients took part in the French AVCnn cohort study, which follows 100 term-born children suffering from NAIS (Chabrier et al., 2010; Husson et al., 2010). The diagnosis was based on the 2007 definition of NAIS: 1) acute neurological symptoms within the first 28 days of life, 2) accompanied by correlated imaging findings, i.e. ischemic lesion in an arterial territory (Raju et al., 2007). All children were enrolled in 37 French hospitals between November 2003 and October 2006.

The present study is a cross-sectional clinical and imaging analysis at age 7 (Dinomais et al., 2015; Chabrier et al., 2016). 73 children were available for follow-up examinations and 52 for MRI. To ensure a homogeneous distribution of lesion characteristics, only the 38 children with unilateral lesions in the territory of the middle cerebral artery were selected as subjects for this study. Six scans had to be excluded due to severe motion artifacts (Dinomais et al., 2015), leaving 32 participants as the population of our study. 31 term-born, age-matched children with typical development and normal neurological exam were recruited for the healthy control (HC) group.

All patients and their parents gave informed written consent. Approvals from the local ethics committees were obtained.

Manual dexterity for both the ipsi- and contralesional hand was measured by the Box and Blocks Test (BBT). For this test, subjects are presented with a box of standardized dimensions, divided into two compartments by a separating wall. Subjects are then asked to transfer wooden blocks from one compartment into the other using one hand. The test score is defined as the number of correctly transferred blocks within one minute. This tool has been validated for the assessment of unilateral gross manual dexterity in children (Mathiowetz et al., 1985). HC were not tested for BBT.

2.2. Image acquisition and lesion delineation

All MRI acquisitions were performed on a 3.0 Tesla scanner (MAGNETOM Trio Tim system, Siemens, Erlangen, Germany) using a 12 channel head coil, at Neurospin, CEA-Saclay, France. Imaging sequences included a high-resolution 3D T1-weighted volume, a 3D FLAIR sequence, and a diffusion-weighted dual SE-EPI sequence with 30 diffusion encoding gradient directions using a b -value of 1000 s/mm² and isotropic voxels of 1.8x1.8x1.8 mm³. Further sequence details are documented in previous work (Dinomais et al., 2015).

Lesions were delineated separately by two trained pediatric neurologists blinded for clinical information. Binary lesion masks were created using the MRICro software (<https://people.cas.sc.edu/rorden/mricro/index.html>) on individual 3D T1 images as well as coregistered 3D FLAIR images and subsequently validated by consensus (Dinomais et al., 2015).

2.3. Preprocessing and FOD calculation

Preprocessing was performed using the open source software MRtrix 3.0 (Tournier et al., 2019) and single-shell 3-tissue constrained spherical deconvolution (SS3T-CSD; Dhollander and Connelly, 2016) was performed using MRtrix3Tissue (<https://3tissue.github.io/>), a fork built on the MRtrix3 framework.

Diffusion MRI data were denoised (Veraart et al., 2016) and corrected for Gibbs ringing (Kellner et al., 2016), subject movement, eddy current-induced artifacts (Andersson and Sotiropoulos, 2015) and bias fields (Tustison et al., 2010). Global intensity normalization was performed to enable quantitative comparisons between subjects (Dhollander et al., 2021b).

Individual and cohort-averaged tissue response functions for Grey Matter (GM), cerebrospinal fluid, and single-fiber WM compartments were calculated (Dhollander et al., 2016) and used to compute WM Fiber Orientation Distribution (FOD) functions within the healthy tissue of each subject. The latter step was performed using SS3T-CSD (Dhollander and Connelly, 2016).

2.4. Fixel-based analysis (FBA)

To enable comparisons of individual fiber populations in each voxel across groups, a study-specific FOD template was generated from the control group FOD images using an iterative nonlinear registration and averaging approach (Raffelt et al., 2011; Raffelt et al., 2012). Patient FOD images were not included in the template generation to prevent introducing anatomical irregularities from the lesion areas. In the resulting FOD template, fixels were automatically segmented to serve as the common fixel analysis mask for further fixel analyses (Dhollander et al., 2021a).

For each subject, fixels and their associated FD values were calculated from the respective FOD image in subject space (Dhollander et al., 2021a). Subject FOD images were then nonlinearly registered to the study-specific FOD template. A fixel analysis mask was derived from the FOD template (by segmenting the FOD lobes) and subject-wise fixels were reoriented and assigned to corresponding fixels of the fixel analysis mask to enable fixel-wise comparison between subjects in template space. Fixel-wise FC values for all subjects were derived from the warp fields from the respective subject space into template space, and log-transformed. The aforementioned steps are typical for a state-of-the-art FBA pipeline (Raffelt et al., 2017; Dhollander et al., 2021a).

Fixels with altered FD, FC, or FDC were identified in a whole-brain FBA over all healthy WM fixels. Using the union of all subject lesion masks in template space as a common lesion mask, all lesional tissue was excluded from the analysis, i.e. only fixels from voxels which had been classified as non-lesioned for all patients were included in the analysis. As recommended for whole-brain FBA, Left Lesioned Patients (LLP) and Right Lesioned Patients (RLP) were compared against HC in separate analyses (Dhollander et al., 2021a). Based on the framework of connectivity-based fixel enhancement (Raffelt et al., 2015), statistical inference was performed for each fixel using a general linear model and non-parametric permutation testing over 5000 permutations (Nichols and Holmes, 2001). Nuisance variables included sex for FD, and sex and intracranial volume for FC and FDC comparisons. Significance was determined at a FWE-corrected $p < 0.05$. MRtrix3 (Tournier et al., 2019) was used to perform the statistical analyses and generate visualizations of the results.

2.5. Tract-wise analysis of interhemispheric connections

A GM parcellation was obtained by registering the HCP MMP 1.0 atlas (Glasser et al., 2016) onto the common study FOD template using the Freesurfer suite v6.0.0 (<https://surfer.nmr.mgh.harvard.edu/>) and ANTs (Avants et al., 2011). Subsequently, the primary motor (M1) and primary sensory cortex (S1), the supplementary motor area (SMA), the

premotor cortex (PMC) as well as the parietal cortex were defined on this atlas by merging regions as detailed in Supplementary Document 1. Furthermore, the temporal and occipital cortex were defined manually within the group template.

For the purpose of segmenting the interhemispheric connections across the CC, we reused the tractogram that was formerly generated to calculate local fixel connectivity information in the FBA analysis. This is a whole-brain probabilistic tractogram, seeded whole-brain in the FOD template itself, consisting of 2 million streamlines, as is customary for a typical FBA pipeline (Raffelt et al., 2017; Dhollander et al., 2021a).

For each selected cortical region, streamlines connecting the equivalent regions in the right and left hemispheres across the CC were then extracted from this whole-brain tractogram. Spurious, anatomically implausible streamlines were removed. Where required, additional exclusion regions were drawn manually to exclude larger, aberrant bundles of streamlines. For each interhemispheric tract, mean FD, FC and FDC values were calculated across all fixels within healthy tissue along the respective tracts streamlines. A 3D visualization of all interhemispheric tract definitions is included in the supplementary materials (Video 1).

Statistical analysis of mean fixel metrics across interhemispheric tracts was performed for the combined group of LLP and RLP against HC, using an ANCOVA with sex as covariate for FD, and sex and intracranial volume for FC and FDC comparisons. Bonferroni correction was applied for the number of tracts included in the analysis.

After obtaining results for group differences in mean FDC in callosal tracts, correlation between patient BBT scores for the ipsi- and contralesional hand, and mean fixel metrics in callosal tracts with significant differences, was calculated using Spearman's rank correlation coefficient. Significance was determined at $p < 0.05$.

Tract averaged statistics and visualizations were created using the R language framework (R Core Team, 2017) with the tidyverse (Wickham et al., 2019) and ggplot2 libraries (Wickham, 2009).

The raw and processed data required to reproduce all of the above findings cannot be shared at this time due to legal and ethical reasons.

3. Results

Demographic and clinical features of our cohort are presented in Table 1. No significant differences between groups were observed in sex, lesion volume or BBT scores.

The low percentage of right-handed children in LLP (33% vs 93% in RLP and 90% in HC) might be due to altered hand preference following the ischemic insult of the dominant hemisphere controlling the right hand (Dinomais et al., 2017). Likewise, the differences in total intracranial volume (HC: mean TIV of 1398 ml vs 1304 ml in LLP and 1274

Table 1

Demographic details of the study cohort. Data presentation is mean (SD), median (IQR) or number (%). HC: Healthy controls, LLP: Left lesioned patients, RLP: Right lesioned patients, TIV: Total intracranial volume, BBT: Box-and-Blocks-Test, SD: Standard deviation, IQR: Interquartile range. p -values are obtained by Kruskal-Wallis non-parametric H-test. a: Chi-squared test.

	HC (n = 31)	LLP (n = 18)	RLP (n = 14)	p -value
Males	16 (52%)	10 (56%)	9 (64%)	0.73 a
Age [years] (SD)	7.7 (0.6)	7.4 (0.5)	7.3 (0.4)	0.543
Right handed	28 (90%)	6 (33%)	13 (93%)	< 0.001 a
TIV [ml] (SD)	1398 (109)	1304.1 (147.9)	1274.6 (101.2)	0.005
Lesion volume [ml] (IQR)	–	27.5 (4.7 – 63.9)	14.7 (4.7–68.2)	0.88
BBT ipsilesional (IQR)	–	32.5 (27.25–38.75)	32 (31–34)	0.95
BBT contralesional (IQR)	–	30 (26.5–37.75)	27 (23.5–31)	0.46

ml in RLP) are explained by volume reductions of the affected hemisphere as a consequence of the ischemic insult.

3.1. Fixel-based analysis

Several regions of significantly reduced fiber density (FD) and (combined) fiber density and cross-section (FDC) were found in both LLP and RLP in comparison to HC, and are depicted in Fig. 1. The affected areas were located mainly in the parietal and temporal WM, as well as in the posterior CC.

In LLP, the bulk of the results was found arching from the parietal

into the temporal WM, encompassing parts of the ipsilateral fornix and the parietal segment of the superior longitudinal fasciculus. Major parts of affected fixels were located in close vicinity to the common lesion mask or the posterior body of the left lateral ventricle. Here, FDC was reduced up to 35% in comparison to HC. Additionally, three small, distinct areas of FDC reductions of up to 55% were found leading towards parietal cortical areas VIP, TE1P and PHT (corresponding to the HCP MMP atlas).

FD reductions in LLP encompassed similar areas as FDC alterations, with up to 40% relative reduction of FD in comparison to HC. Additional, more extensive ipsilesional areas of reduced FD of up to 35%

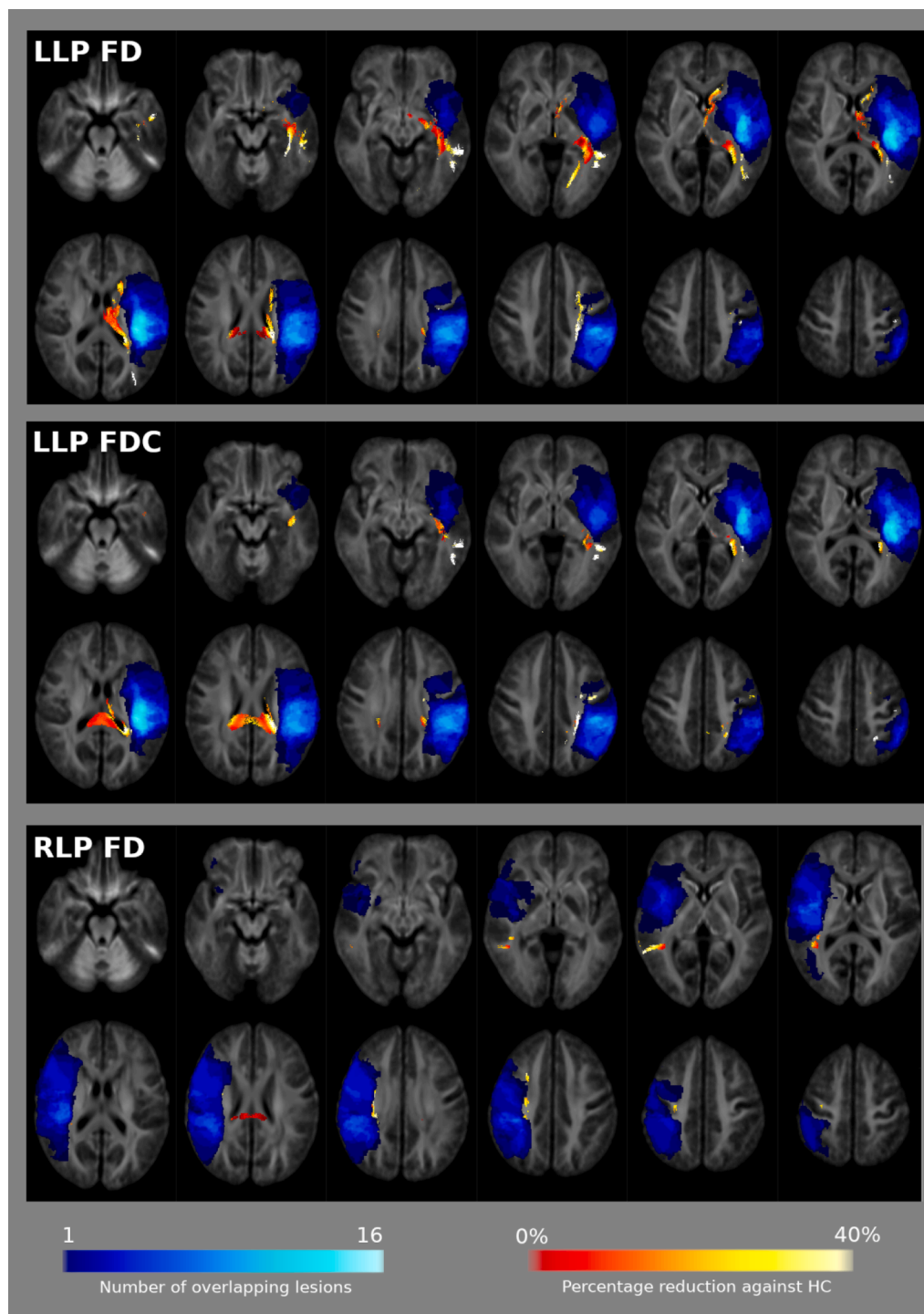


Fig. 1. White matter alterations, as detected in the whole-brain fixel-based analysis. Fixels with significantly reduced metrics (ANCOVA, FWE-corrected $p < 0.05$) for left lesion patients (LLP) fiber density (FD) and fiber density and cross-section (FDC), and right lesion patients (RLP) FD, overlaid on the group template. Fixels colored by percentage decrease in comparison to healthy controls. Ancova covariates: subject sex for FD, sex and intracranial volume for FDC. Blue scale: Lesion distribution. The union of all subject lesions was used as the common lesion mask for the fixel-based analysis. Not shown: LLP and RLP Fiber Cross-Section and RLP FDC, as no significant alterations were detected. (For interpretation of the references to colour in this figure legend, the reader is referred to the web version of this article.)

were found arching anteriorly along the fornix and posteriorly towards the primary visual cortex.

In RLP, while alterations were also observed in parietal and temporal WM, reductions were significant only in FD, and affected areas were considerably smaller than in LLP. A cluster of FD reductions of up to 50% was observed in the right SLF near the common lesion mask, another one in the right inferior parietal lobe, leading towards areas TE1p and PHT in the atlas.

In the isthmus and anterior splenium of the Corpus Callosum (CC), both LLP and RLP showed a cluster of altered fixels. LLP exhibited reductions in FD of up to 15% and reductions in FDC of up to 25% in comparison to HC. In RLP, FD reductions of up to 20% within the isthmus of the CC were spatially less extensive, while FDC reductions of up to 20% did not reach significance. Detailed illustrations of CC involvement can be found in Fig. 2.

Fiber cross-section (FC) demonstrated extensive alterations when including only sex as a covariate. However, none of these differences remained significant when introducing intracranial volume as a covariate of non-interest. This indicates those FC alterations were only a trivial effect related to the overall volume of the intracranial space.

We did not find any areas of altered fixel-wise metrics within the contralesional hemispheres of either LLP or RLP outside the affected CC regions. Also, we found no fixels with significantly increased FD, FC or FDC in patients in comparison to HC.

3.2. Analysis of interhemispheric connections

Comparison of tract-averaged fixel metrics using an ANCOVA with

the same covariates of non-interest as in the fixel-based analysis revealed significant differences for FC in the S1 connection, in FD in the SMA, parietal, temporal, and occipital connections, and for FDC in the SMA, parietal and temporal interhemispheric connections. After Bonferroni-correction for the number of investigated tracts, differences remained significant in FD in parietal, temporal, and occipital connections, as well as in FDC in parietal connections. Mean tract FDC values and ANCOVA results are illustrated in Fig. 2, with additional plots for FD and FC available in supplementary document 2.

Using Spearman's rank-correlation coefficient, we found significant correlations of mean FDC with the contralesional BBT score in all interhemispheric tracts with significantly reduced FDC. Furthermore, mean FDC in the SMA interhemispheric connection was also found to be significantly correlated with the ipsilesional BBT score. FC produced similar results to those found to FDC, while FD exhibited only a significant correlation with contralesional BBT in the temporal callosal tract. The results for FDC, together with their respective ρ and p values, are illustrated in Fig. 3. Additional figures for FD and FC are provided in supplementary document 2.

4. Discussion

In this study, an advanced fixel-based analysis (FBA) of diffusion MRI demonstrates that 7 years after NAIS of the middle cerebral artery (MCA), affected children show WM tissue alterations in brain networks distant from the original area of the ischemic lesion. While at this age the lesion site has reorganized as gliotic tissue, the surrounding tissue appears normal upon visual inspection of conventional MRI. However, FBA

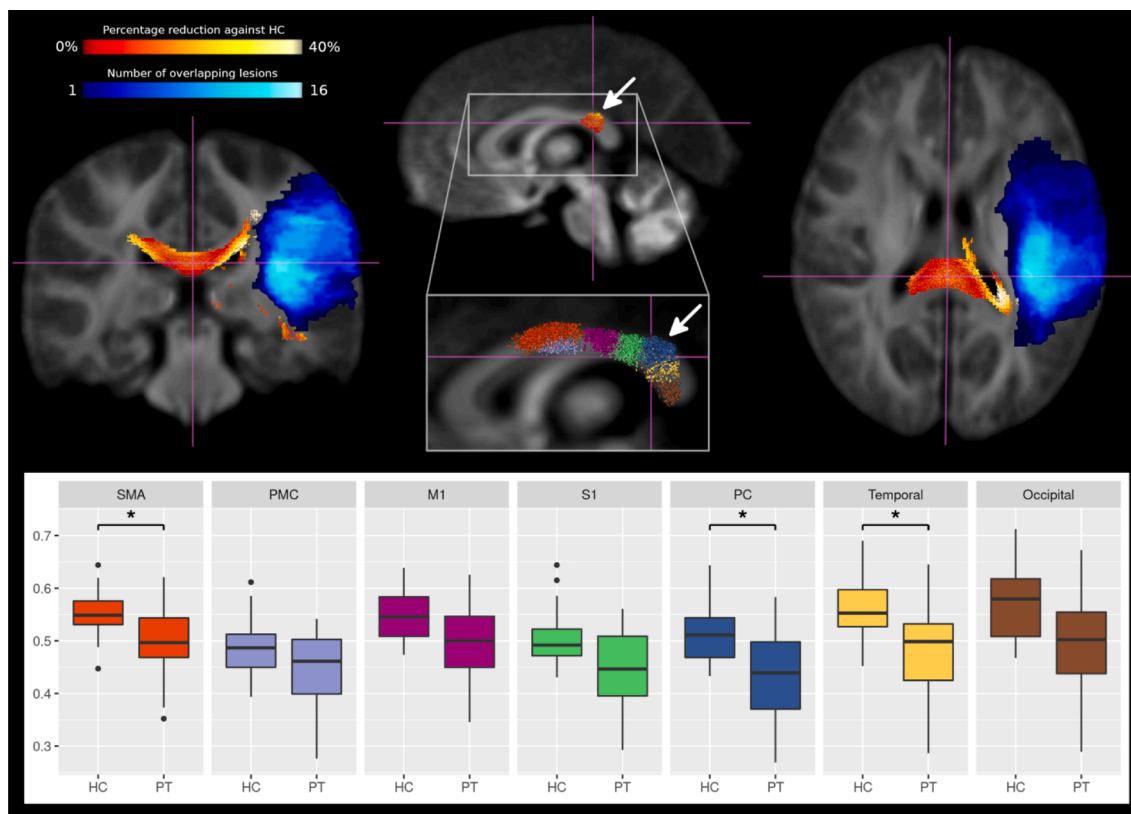


Fig. 2. White matter alterations in interhemispheric connections. **Top:** Results of fixel-based analysis (FBA) in coronal, sagittal and axial view. Fixels with significantly reduced Fiber Density and Cross-section (FDC; FWE-controlled $p < 0.05$) in left lesioned patients (LLP), colored by percentage reduction against healthy controls (HC), overlaid on the group template. Blue scale: Lesion distribution. **Magnified:** Midsagittal view of the corpus callosum, overlaid with streamlines of interhemispheric connections. Streamline colors correspond to those from the boxplots. The white arrow indicates the location of altered fixels in the FBA. **Bottom:** Comparison of mean FDC in interhemispheric tracts between HC and patients (PT) in an ANCOVA with sex, age and intracranial volume as covariates of non-interest. SMA, PC and Temporal interhemispheric connections show significant reduction of mean FDC. (For interpretation of the references to colour in this figure legend, the reader is referred to the web version of this article.)

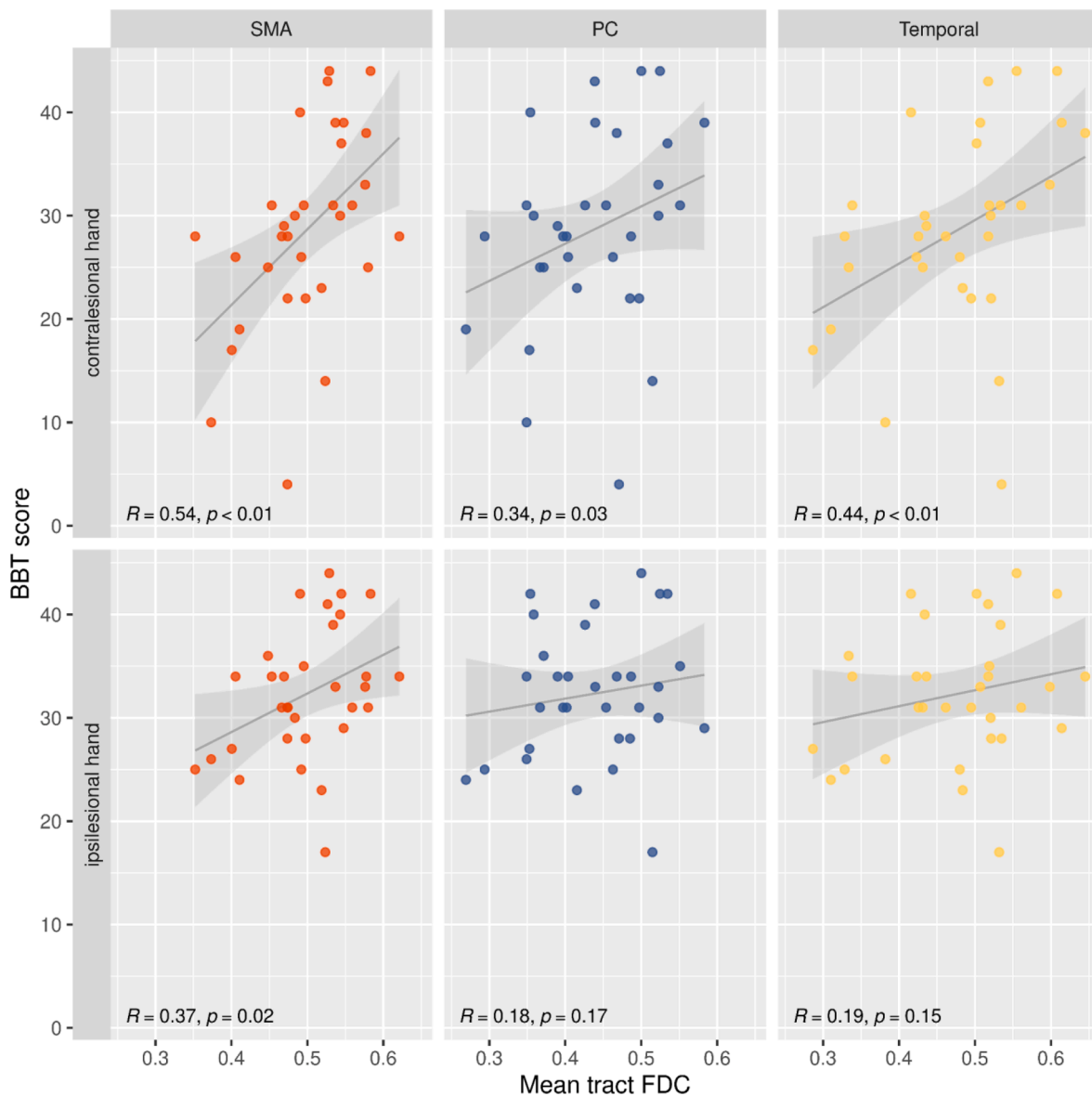


Fig. 3. Correlation of mean tract Fiber density and cross-section (FDC, x-axis) and manual dexterity (BBT score, y-axis) of the contralesional (affected, top row) and ipsilesional (non-affected, bottom row) hand for interhemispheric tracts with significantly reduced FDC (see Fig. 2). Spearman rank-correlation Rho and p value, as well as linear regression lines, are shown per combination. Mean FDC in all these interhemispheric connections is significantly correlated to contralesional manual dexterity. Additionally, the connection between the left and right Supplementary Motor Area (SMA) show significant correlation of mean FDC with ipsilesional manual dexterity. Colors correspond to Fig. 2. SMA: Supplementary Motor Area. PC: Parietal Cortex.

reveals fiber-specific differences between patients and healthy controls in WM microstructure within the normal-appearing tissue, which explain functional deficits in these children.

The whole-brain approach of FBA allows for an investigation of WM alterations throughout the entire WM, without being restricted to predefined regions of interest. In this way, the majority of affected fixels were found in WM within the parietal and temporal lobe of the affected hemisphere, as well as within the interhemispheric connections between these lobes across the CC. Furthermore, tract-averaged fixel metrics across interhemispheric tracts within the CC were shown to correlate with gross manual dexterity of the affected, contralesional hand, supporting the functional relevance of these observations. Our findings thus underline that early unilateral focal lesions within WM and GM cause long-lasting injuries within connected structures remote from the infarct site.

Our results fall within the realm of diaschisis, a concept dating back to the early 20th century when von Monakov introduced the term to

describe neurological morbidity distant from the site of a focal brain lesion (Carrera and Tononi, 2014). To our knowledge, no previous publications have used FBA to explore long-term diaschisis in children after NAIS. However, previous publications used voxel-based approaches to investigate diaschisis after MCA AIS in newborns (Srivastava et al., 2019, 18 subjects) and children (Kirton et al., 2016, 19 subjects) in the days immediately following the ischemic insult. Although limited by small cohort sizes, these studies report reduced diffusivity in the thalamus and the CC. Our results corroborate these findings, suggesting that we might have detected the long-term outcomes of these early observations.

Long term WM alterations have also been explored in children with unilateral cerebral palsy caused by a wider range of WM lesions (Mailleux et al., 2020). The majority of studies investigated DTI metrics within predetermined ROIs or fiber tracts, most commonly the CST. The small number of studies based on a whole-brain approach, however, found alterations within a considerably larger number of WM structures.

Notable overlaps to our findings include thalamic radiations (Arrigoni et al., 2016; Pannek et al., 2014) and the posterior corpus callosum (Arrigoni et al., 2016). In addition to being consistent with our findings of perithalamic and interhemispheric WM alterations, this highlights the added value of whole-brain approaches in revealing a more comprehensive picture of non-trivial lesion effects throughout the brain than ROI-based methods.

In contrast to previous work on this cohort (Dinomais et al., 2015), the FBA did not detect significant alterations of fixel metrics in the ipsilesional CST. The most likely reason for this observation is the rigorous controlling for the family-wise error rate implemented in the statistical method underlying FBA. The relatively mild impairment of manual dexterity in both LLP and RLP, which has been shown to correlate with DTI metrics in chronic stroke (Lindenberg et al., 2010), might have further contributed to this observation. Taken together, these factors are likely to have caused the differences in CST fixel metrics to fall below the significance threshold in our analysis, while an isolated investigation of the ipsilesional CST revealed altered DTI metrics (Dinomais et al., 2015). This demonstrates the benefit of fixel-based analysis in investigating the entire WM and identifying the most prominent alterations, as opposed to focused analyses of individual areas.

Previous work with this cohort has provided evidence for alterations of structural parameters and possible compensatory processes in the contralesional hemisphere after NAIS, and also suggested that lesion lateralization might influence subsequent brain development (Al Harrach et al., 2019). Such processes might also manifest in structural connectivity within the CC, given that it connects the hemispheres and enables transfer of information (Gazzaniga, 2000). We therefore complemented the FBA with an analysis of tract-averaged fixel metrics specifically within the CC.

The involvement of the isthmus and anterior splenium of the CC is readily visible in the WBA (see Fig. 2). The tract-averaged analysis reveals these sections to be composed mainly by fibers connecting the parietal and temporal cortex, which also exhibit significantly reduced fixel metrics. This is in accordance with earlier anatomical investigations (De Lacoste et al., 1985). Regarding the functional significance of these observations, mean FDC in these interhemispheric connections exhibited significant associations with contralesional BBT scores. Associations of other diffusion-based metrics within these connections with motor function have previously been described (Kurth et al., 2013), however, similar correlations were also found with speech production (Friederici et al., 2007) as well as with auditory function and speech perception (Westerhausen et al., 2009). At the same time, hand motor function was found to be related to a multitude of CC sections (Groeschel et al., 2017; Hawe et al., 2013; Fling and Seidler, 2012). While our results add further evidence for the association of these connections with gross manual dexterity, the multitude of reported functional associations illustrates the challenge of localizing function within the CC (Gooijers and Swinnen, 2014). The tract-averaged analysis of CC tracts also revealed significant reductions of fixel-wise metrics within the connection between left and right SMA (see Fig. 2). Moreover, a significant, moderate to strong correlation of average FDC with the BBT scores for both the affected and the non-affected hand was found for this connection, demonstrating functional relevance for gross manual dexterity (see Fig. 3). This observation appears to be related to analyses of functional activation after stroke (Grefkes and Ward, 2014). Changes in functional activation within the motor network after ischemic lesions have been shown to involve cortical areas within the contralesional hemisphere, including the SMA (Grefkes and Ward, 2014). Furthermore, the amount and distribution of abnormal functional activation was found to change during the weeks and months after the insult, with good motor recovery depending on reinstatement of original ipsilesional activation patterns, while sustained overactivation in the contralesional primary motor cortex was detrimental to long-term motor function (Rehme et al., 2012).

However, for the contralesional SMA, greater activation likelihood was related to better hand motor performance after stroke, indicating a compensatory role of this cortical area (Rehme et al., 2012). Our results of increased FDC within the interhemispheric connection between left and right SMA being correlated with better manual dexterity after NAIS provide the structural correlate to these findings from the functional domain. As FDC is likely related to the capacity of WM fiber tracts to transfer information (Raffelt et al., 2017), our findings show that not only activation of the contralesional SMA, but also the ability to exchange information between left and right SMA, is associated with manual dexterity after NAIS. Previous studies have related the connection between left and right SMA to bimanual coordination skills (Johansen-Berg et al., 2007) and mirror movements (Hawe et al., 2013). We can thus extend these observations, further underlining the importance of both the ipsi- and contralesional SMA and their interhemispheric connection for recovery of manual dexterity after NAIS.

Outside the interhemispheric fiber pathways, we did not observe altered fixel metrics in the contralesional hemisphere. We also did not find areas with significantly increased fixel metrics in either the FBA or the tract-averaged analysis. Such findings might have corroborated previous works reporting compensatory processes in the non-affected WM after NAIS (Al Harrach et al., 2021; Al Harrach et al., 2019). However, analogous to the above discussion on the absence of significant alterations in the CST, this observation might be explained by the strict control for the family-wise error rate, potentially suppressing smaller effects from reaching significance.

Across all fixel-wise metrics, alterations in LLP were more extensive than in RLP. A similar effect was observed in previous work (Al Harrach et al., 2021; Al Harrach et al., 2019), corroborating that in the present cohort, LLP are indeed more strongly affected. A possible interpretation could be that brain adaptation and possible subsequent reorganization are sensitive to the side of the lesion, given the functional asymmetry between hemispheres. Another explanation might relate to the differences in lesion localization between RLP and LLP, which in LLP were more concentrated in the pre- and postcentral gyri, while lesions in RLP were distributed across the MCA territory more evenly (see Fig. 1), possibly leading to a statistically stronger and more easily detected effect in LLP.

It seems likely that the observed alterations share a common underlying pathophysiological mechanism, given that the results in the present study were all observed near or in structures strongly connected to the lesioned area. As NAIS disrupts the very dynamic WM maturation processes within the first years of life (Lebel et al., 2019), it appears as if subsequent development and maturation was unable to compensate for the disruptions from the primary ischemic incident. Previous publications have proposed Wallerian degeneration originating from the focal lesion (Dinomais et al., 2016; Husson et al., 2010) or altered conditions within the MCA flow region (Husson et al., 2016; Steiner et al., 2021); as possible explanations for observed tissue changes after NAIS. This would be supported by our findings of significant changes in FD and FDC indicating microstructural tissue changes, while FC did not reach significance after incorporating total intracranial volume as a covariate of non-interest, therefore suggesting that macrostructural differences on the fixel level were proportional to intracranial volume. However, such a straightforward interpretation is complicated by the intricate relation of the three FBA metrics (Dhollander et al., 2021a), especially given the limited *b*-value available in our diffusion MRI sequence, which, while sufficient for detecting significant FD effects, is at the lower end of what can be considered sufficient for the assumptions underlying apparent fiber density to hold in an FBA (Dhollander et al., 2021a). Moreover, while great care was taken to ensure good registration results, the presence of focal lesions unavoidably introduces irregularities during registration which might further blur the distinction between FD and FC (Dhollander et al., 2021a). For this reason, although our results point towards microstructural alterations in intra-axonal volume as the biological process underlying the observed results, drawing strong

conclusions from the observed distribution of results between FD and FC would be premature, with future studies required to further elucidate these questions.

5. Limitations

Certain limitations must be acknowledged. Because FBA had to be performed separately for LLP and RLP as suggested in [Dhollander et al. \(2021a\)](#), no additional stratification for further clinical parameters was possible due to the relatively small sample size. At the same time, our study cohort was comparable in size to other studies investigating NAIS using advanced MRI. Also, as discussed above, our b-value was limited, which renders the FD results potentially slightly less specific to intra-axonal effects due to the presence of some extra-axonal signal.

6. Conclusion

In conclusion, our results show that seven years after NAIS, affected children still show WM tissue differences in comparison to healthy controls. Affected areas include the temporal and parietal WM as well as interhemispheric connections across the CC, the latter of which correlate significantly with gross manual dexterity of the affected hand. Furthermore, the connection between left and right SMA appears to be associated with long-term manual dexterity. The specific strength of this study stems from the well-defined study cohort of children after unilateral NAIS of the MCA, as well as from the whole-brain, fixel based analysis approach, which allows for a fiber-specific, yet comprehensive investigation of the long-term effects of NAIS on the entire WM.

CRediT authorship contribution statement

Pablo Pretzel: Investigation, Formal analysis, Visualization, Data curation, Writing – original draft. **Thijs Dhollander:** Methodology, Software, Writing – review & editing, Supervision. **Stéphane Chabrier:** Conceptualization, Resources, Writing – review & editing, Supervision. **Mariam Al-Harrach:** Resources, Writing – review & editing. **Lucie Hertz-Pannier:** Conceptualization, Resources, Writing – review & editing. **Mickaël Dinomais:** Conceptualization, Resources, Writing – review & editing, Funding acquisition, Supervision. **Samuel Groeschel:** Conceptualization, Funding acquisition, Writing – review & editing, Supervision.

Declaration of Competing Interest

The authors declare that they have no known competing financial interests or personal relationships that could have appeared to influence the work reported in this paper.

Acknowledgements

We would like to express our gratitude to all members of the AVCnn group for their contribution to this ongoing project. Funding PP was supported by the IZKF Promotionskolleg of the Faculty of Medicine, University Tuebingen (2018-1). The research was supported by the University Hospital of Angers (eudract number 2010A00976-33), the Ministère de la solidarité et de la santé (eudract number 2010-A0032930), and the Fondation de l'Avenir (ET0-571).

Appendix A. Supplementary data

Supplementary data to this article can be found online at <https://doi.org/10.1016/j.nicl.2022.103035>.

References

- Aa, Niek E. van der, Frances J. Northington, Brian S. Stone, Floris Groenendaal, Manon J. N. L. Benders, Giorgio Porro, Shoko Yoshida, Susumu Mori, Linda S. de Vries, and Jiangyang Zhang. 2013. Quantification of white matter injury following neonatal stroke with serial DTI. *Pediatric Res.* 73 (6, 6): 756–62. [10.1038/pr.2013.45](https://doi.org/10.1038/pr.2013.45).
- Harrach, A.L., Mariam, P.P., Groeschel, S., Rousseau, F., Dhollander, T., Hertz-Pannier, L., Lefevre, J., Chabrier, S., Dinomais, M., AVCnn Study Group, 2021. A connectome-based approach to assess motor outcome after neonatal arterial ischemic stroke. *Ann. Clin. Transl. Neurol.*, March. <https://doi.org/10.1002/acn3.51292>.
- Harrach, A.L., Mariam, F.R., Groeschel, S., Wang, X., Hertz-pannier, L., Chabrier, S., Bohi, A., Lefevre, J., Dinomais, M., 2019. Alterations in cortical morphology after neonatal stroke: compensation in the contralesional hemisphere? *Developm. Neurobiol.* 79 (4), 303–316. <https://doi.org/10.1002/dneu.22679>.
- Arrigoni, F., Peruzzo, D., Gagliardi, C., Maghini, C., Colombo, P., Servodio Iammarrone, F., Pierpaoli, C., Triulzi, F., Turconi, A.C., 2016. Whole-Brain DTI assessment of white matter damage in children with bilateral cerebral palsy: evidence of Involvement Beyond the Primary Target of the Anoxic Insult. *Am. J. Neuroradiol.* 37 (7), 1347–1353. <https://doi.org/10.3174/ajnr.A4717>.
- Avants, B.B., Tustison, N.J., Song, G., Cook, P.A., Klein, A., Gee, J.C., 2011. A Reproducible evaluation of ANTs similarity metric performance in brain image registration. *NeuroImage* 54 (3), 2033–2044. <https://doi.org/10.1016/j.neuroimage.2010.09.025>.
- Carrera, E., Tononi, G., 2014. Diaschisis: past, present, future. *Brain* 137 (9), 2408–2422. <https://doi.org/10.1093/brain/awu101>.
- Chabrier, S., Peyric, E., Drutel, L., Deron, J., Kossorotoff, M., Dinomais, M., Lazaro, L., et al., 2016. Multimodal outcome at 7 years of age after neonatal arterial ischemic stroke. *J. Pediatrics* 172 (May), 156–161.e3. <https://doi.org/10.1016/j.jpeds.2016.01.069>.
- Chabrier, S., Saliba, E., Tich, S.N.T., Charollais, A., Varlet, M.-N., Tardy, B., Presles, E., et al., 2010. Obstetrical and neonatal characteristics vary with birthweight in a cohort of 100 term newborns with symptomatic arterial ischemic stroke. *Eur. J. Paediatric Neurol.* 14 (3), 206–213. <https://doi.org/10.1016/j.ejpn.2009.05.004>.
- Craig, B.T., Hilderley, A., Kinney-Lang, E., Long, X., Carlson, H.L., Kirton, A., 2020. Developmental neuroplasticity of the white-matter connectome in children with perinatal stroke. *Neurology*. <https://doi.org/10.1212/WNL.00000000000010669>.
- De Lacoste, M., Christine, J.B., Kirkpatrick, Ross, E.D., 1985. Topography of the human corpus callosum. *J. Neuropathol. Exp. Neurol.* 44 (6), 578–591. <https://doi.org/10.1097/00005072-198511000-00004>.
- Dhollander, T., Connelly, A., 2016. A novel iterative approach to reap the benefits of multi-tissue CSD from just single-shell (+ B = 0) diffusion MRI data. *Proc ISMRM 24*, 3010.
- Dhollander, T., Clemente, A., Singh, M., Boonstra, F., Civier, O., Dominguez, J.F., Natalia Egorova, D., et al., 2021a. Fixel-based analysis of diffusion MRI: methods, applications, challenges and opportunities. *NeuroImage* 241, 118417. <https://doi.org/10.1016/j.neuroimage.2021.118417>.
- Dhollander, Thijs, Rami Tabbara, Jonas Rosnarho-Tornstrand, Jacques-Donald Tournier, David Raffelt, Alan Connelly. 2021b. Multi-tissue log-domain intensity and inhomogeneity normalisation for quantitative apparent fibre density.
- Dinomais, M., Hertz-Pannier, L., Groeschel, S., Chabrier, S., Delion, M., Husson, B., Kossorotoff, M., Renaud, C., Nguyen, S., The Tich, VCnn Study Group, A., 2015. Long term motor function after neonatal stroke: lesion localization above all. *Hum. Brain Mapp.* 36 (12), 4793–4807. <https://doi.org/10.1002/hbm.22950>.
- Dinomais, M., Hertz-Pannier, L., Groeschel, S., Delion, M., Husson, B., Kossorotoff, M., Renaud, C., Chabrier, S., The Tich, S.N., VCnn Study Group, A., 2016. Does contralesional hand function after neonatal stroke only depend on lesion characteristics? *Stroke* 47 (6), 1647–1650. <https://doi.org/10.1161/STROKEAHA.116.013545>.
- Dinomais, M., Thébault, G., Hertz-Pannier, L., Gautheron, V., Tich, S.N.T., Fluss, J., Chabrier, S., 2017. Is there an excess of left-handedness after neonatal stroke? *Cortex* 96 (November), 161–164. <https://doi.org/10.1016/j.cortex.2017.08.007>.
- Dunbar, Mary, Aleksandra Mineyko, Michael Hill, Jacquie Hodge, Amalia Floer, Adam Kirton. 2020. Population based birth prevalence of disease-specific perinatal stroke. *Pediatrics* 146 (5). [10.1542/peds.2020-013201](https://doi.org/10.1542/peds.2020-013201).
- Natalia, E., Thijs, D., Salah, K.M., Wasim, K., Emilio, W., Amy, B., 2020. Pervasive white matter fiber degeneration in ischemic stroke. *Stroke* 51 (5), 1507–1513. <https://doi.org/10.1161/STROKEAHA.119.028143>.
- Fling, B.W., Seidler, R.D., 2012. Fundamental differences in callosal structure, neurophysiologic function, and bimanual control in young and older adults. *Cereb. Cortex* 22 (11), 2643–2652. <https://doi.org/10.1093/cercor/bhr349>.
- Fluss, J., Dinomais, M., Chabrier, S., 2019. Perinatal stroke syndromes: similarities and diversities in aetiology, outcome and management. *Eur. J. Paediatric Neurol.* EJPn 23 (3), 368–383. <https://doi.org/10.1016/j.ejpn.2019.02.013>.
- Friederici, A.D., Yves von Cramon, D., Kotz, S.A., 2007. Role of the corpus callosum in speech comprehension: interfacing syntax and prosody. *Neuron* 53 (1), 135–145. <https://doi.org/10.1016/j.neuron.2006.11.020>.
- Gazzaniga, M.S., 2000. Cerebral specialization and interhemispheric communication: does the corpus callosum enable the human condition? *Brain* 123 (7), 1293–1326. <https://doi.org/10.1093/brain/123.7.1293>.
- Glasser, M.F., Coalson, T.S., Robinson, E.C., Hacker, C.D., Harwell, J., Yacoub, E., Ugurbil, K., et al., 2016. A multi-modal parcellation of human cerebral cortex. *Nature* 536 (7615), 171–178. <https://doi.org/10.1038/nature18933>.
- Gooijers, J., Swinnen, S.P., 2014. Interactions between brain structure and behavior: the corpus callosum and bimanual coordination. *Neurosci. Biobehav. Rev.* 43 (June), 1–19. <https://doi.org/10.1016/j.neubiorev.2014.03.008>.

- Grefkes, C., Ward, N.S., 2014. Cortical Reorganization after stroke: how much and how functional? *Neuroscientist* 20 (1), 56–70. <https://doi.org/10.1177/1073858413491147>.
- Groeschel, S., Hertz-Pannier, L., Delion, M., Loustau, S., Husson, B., Kossorotoff, M., Renaud, C., Tich, S.N.T., Chabrier, S., Dinomais, M., 2017. Association of transcallosal motor fibres with function of both hands after unilateral neonatal arterial ischemic stroke. *Dev. Med. Child Neurol.* 59 (10), 1042–1048. <https://doi.org/10.1111/dmcn.13517>.
- Hawe, R.L., Sukal-Moulton, T., Dewald, J.P.A., 2013. The effect of injury timing on white matter changes in the corpus callosum following unilateral brain injury. *NeuroImage Clin.* 3, 115–122. <https://doi.org/10.1016/j.nicl.2013.08.002>.
- Husson, B., Hertz-Pannier, L., Adamsbaum, C., Renaud, C., Presles, E., Dinomais, M., Kossorotoff, M., Landrieu, P., Chabrier, S., 2016. MR angiography findings in infants with neonatal arterial ischemic stroke in the middle cerebral artery territory: a prospective study using circle of willis MR angiography. *Eur. J. Radiol.* 85 (7), 1329–1335. <https://doi.org/10.1016/j.ejrad.2016.05.002>.
- Husson, Béatrice, Hertz-Pannier, L., Renaud, C., Allard, D., Presles, E., Landrieu, P., Chabrier, S., the AVCnn Group, 2010. Motor outcomes after neonatal arterial ischemic stroke related to early MRI data in a prospective study. *Pediatrics* 126 (4), e912–e918. <https://doi.org/10.1542/peds.2009-3611>.
- Johansen-Berg, H., Della-Maggiore, V., Behrens, T.E.J., Smith, S.M., Paus, T., 2007. Integrity of white matter in the corpus callosum correlates with bimanual coordination skills. *NeuroImage* 36 (January), T16–T21. <https://doi.org/10.1016/j.neuroimage.2007.03.041>.
- Jones, D.K., Knösche, T.R., Turner, R., 2013. White matter integrity, fiber count, and other fallacies: the do's and don'ts of diffusion MRI. *NeuroImage* 73 (June), 239–254. <https://doi.org/10.1016/j.neuroimage.2012.06.081>.
- Kellner, E., Dhital, B., Kiselev, V.G., Reiser, M., 2016. Gibbs-ringing artifact removal based on local subvoxel-shifts. *Magn. Reson. Med.* 76 (5), 1574–1581. <https://doi.org/10.1002/mrm.26054>.
- Kirton, A., Williams, E., Dowling, M., Mah, S., Hodge, J., Carlson, H., Wei, X.-C., Ichord, R., the PedNIHSS Investigators, 2016. Diffusion imaging of cerebral diaschisis in childhood arterial ischemic stroke. *Int. J. Stroke.* <https://doi.org/10.1177/1747493016666089>.
- Kirton, A., deVeber, G., 2013. Life after perinatal stroke. *Stroke* 44 (11), 3265–3271. <https://doi.org/10.1161/STROKEAHA.113.000739>.
- Kurth, F., Mayer, E.A., Toga, A.W., Thompson, P.M., Luders, E., 2013. The right inhibition? callosal correlates of hand performance in healthy children and adolescents callosal correlates of hand performance. *Hum. Brain Mapp.* 34 (9), 2259–2265. <https://doi.org/10.1002/hbm.22060>.
- Lebel, C., Treit, S., Beaulieu, C., 2019. A review of diffusion MRI of typical white matter development from early childhood to young adulthood. *NMR Biomed.* 32 (4), e3778 <https://doi.org/10.1002/nbm.3778>.
- Lee, J., Croen, L.A., Lindan, C., Nash, K.B., Yoshida, C.K., Ferriero, D.M., Barkovich, A.J., Yvonne, W.W., 2005. Predictors of outcome in perinatal arterial stroke: a population-based study. *Ann. Neurol.* 58 (2), 303–308. <https://doi.org/10.1002/ana.20557>.
- Lindenberg, R., Renga, V., Zhu, L.L., Betzler, F., Alsop, D., Schlaug, G., 2010. Structural Integrity of corticospinal motor fibers predicts motor impairment in chronic stroke. *Neurology* 74 (4), 280–287. <https://doi.org/10.1212/WNL.0b013e3181ccc6d9>.
- Mailleux, L., Franki, I., Emsell, L., Peedima, M.-L., Fehrenbach, A., Feys, H., Ortbis, E., 2020. The relationship between neuroimaging and motor outcome in children with cerebral palsy: a systematic review—Part B diffusion imaging and tractography. *Res. Dev. Disabil.* 97 (February), 103569 <https://doi.org/10.1016/j.ridd.2019.103569>.
- Mathiowetz, V., Federman, S., Wiemer, D., 1985. Box and block test of manual dexterity: norms for 6–19 year olds. *Can. J. Occup. Ther.* 52 (5), 241–245. <https://doi.org/10.1177/000841748505200505>.
- Mito, R., Raffelt, D., Dhollander, T., Vaughan, D.N., Donald Tournier, J., Salvado, O., Brodtmann, A., Rowe, C.C., Villemagne, V.L., Connelly, A., 2018. Fibre-specific white matter reductions in Alzheimer's Disease and mild cognitive impairment. *Brain* 141 (3), 888–902. <https://doi.org/10.1093/brain/awx355>.
- Nichols, T.E., Holmes, A.P., 2001. Nonparametric permutation tests for functional neuroimaging: a primer with examples. *Hum. Brain Mapp.*
- Pannek, K., Boyd, R.N., Fiori, S., Guzzetta, A., Rose, S.E., 2014. Assessment of the structural brain network reveals altered connectivity in children with unilateral cerebral palsy due to periventricular white matter lesions. *NeuroImage: Clinical* 5 (January), 84–92. <https://doi.org/10.1016/j.nicl.2014.05.018>.
- Raffelt, D.A., Smith, R.E., Ridgway, G.R., Donald Tournier, J., Vaughan, D.N., Rose, S., Henderson, R., Connelly, A., 2015. Connectivity-based fixel enhancement: whole-brain statistical analysis of diffusion MRI measures in the presence of crossing fibres. *NeuroImage* 117 (August), 40–55. <https://doi.org/10.1016/j.neuroimage.2015.05.039>.
- Raffelt, D.A., Donald Tournier, J., Smith, R.E., Vaughan, D.N., Jackson, G., Ridgway, G.R., Connelly, A., 2017. Investigating white matter fibre density and morphology using fixel-based analysis. *NeuroImage* 144 (January), 58–73. <https://doi.org/10.1016/j.neuroimage.2016.09.029>.
- Raffelt, D., Donald Tournier, J., Frupp, J., Crozier, S., Connelly, A., Salvado, O., 2011. Symmetric diffeomorphic registration of fibre orientation distributions. *NeuroImage* 56 (3), 1171–1180. <https://doi.org/10.1016/j.neuroimage.2011.02.014>.
- Raffelt, D., Donald Tournier, J., Rose, S., Ridgway, G.R., Henderson, R., Crozier, S., Salvado, O., Connelly, A., 2012. Apparent fibre density: a novel measure for the analysis of diffusion-weighted magnetic resonance images. *NeuroImage* 59 (4), 3976–3994. <https://doi.org/10.1016/j.neuroimage.2011.10.045>.
- Raju, T.N.K., Nelson, K.B., Ferriero, D., Lynch, J.K., 2007. Ischemic perinatal stroke: summary of a workshop sponsored by the national institute of child health and human development and the national institute of neurological disorders and stroke. *Pediatrics* 120 (3), 609–616. <https://doi.org/10.1542/peds.2007-0336>.
- R Core Team, 2017. *R: A Language and Environment for Statistical Computing. Manual. R Foundation for Statistical Computing, Vienna, Austria.*
- Rehme, A.K., Eickhoff, S.B., Rottschy, C., Fink, G.R., Grefkes, C., 2012. Activation likelihood estimation meta-analysis of motor-related neural activity after stroke. *NeuroImage* 59 (3), 2771–2782. <https://doi.org/10.1016/j.neuroimage.2011.10.023>.
- Righini, A., Doneda, C., Parazzini, C., Arrigoni, F., Matta, U., Triulzi, F., 2010. Diffusion tensor imaging of early changes in corpus callosum after acute cerebral hemisphere lesions in newborns. *Neuroradiology* 52 (11), 1025–1035. <https://doi.org/10.1007/s00234-010-0745-y>.
- Srivastava, R., Rajapakse, T., Carlson, H.L., Keess, J., Wei, X.-C., Kirton, A., 2019. Diffusion imaging of cerebral diaschisis in neonatal arterial ischemic stroke. *Pediatr. Neurol.* 100 (November), 49–54. <https://doi.org/10.1016/j.pediatrneurol.2019.04.012>.
- Steiner, L., Federspiel, A., Jaros, J., Slavova, N., Wiest, R., Steinlin, M., Grunt, S., Everts, R., 2021. Cerebral blood flow and cognitive outcome after pediatric stroke in the middle cerebral artery. *Sci. Rep.* 11 <https://doi.org/10.1038/s41598-021-98309-w>.
- Tournier, J.-Donald, Robert Smith, David Raffelt, Rami Tabbara, Thijs Dhollander, Maximilian Pietsch, Daan Christiaens, Ben Jeurissen, Chun-Hung Yeh, and Alan Connelly. 2019. MRtrix3: A Fast, Flexible and Open Software Framework for Medical Image Processing and Visualisation. *bioRxiv*, February, 551739. 10.1101/551739.
- Tustison, N.J., Avants, B.B., Cook, P.A., Zheng, Y., Egan, A., Yushkevich, P.A., Gee, J.C., 2010. N4ITK: improved N3 bias correction. *IEEE Trans. Med. Imaging* 29 (6), 1310–1320. <https://doi.org/10.1109/TMI.2010.2046908>.
- Veraart, J., Novikov, D.S., Christiaens, D., Ades-aron, B., Sijbers, J., Fieremans, E., 2016. Denoising of diffusion MRI using random matrix theory. *NeuroImage* 142 (Supplement C), 394–406. <https://doi.org/10.1016/j.neuroimage.2016.08.016>.
- Westerhausen, R., Grüner, R., Specht, K., Hugdahl, K., 2009. Functional relevance of interindividual differences in temporal lobe callosal pathways: a DTI tractography study. *Cereb. Cortex* 19 (6), 1322–1329. <https://doi.org/10.1093/cercor/bhn173>.
- Wickham, H., 2009. *Ggplot2: Elegant Graphics for Data Analysis. Springer-Verlag, New York* <http://ggplot2.org>.
- Wickham, Hadley, Mara Averick, Jennifer Bryan, Winston Chang, Lucy D'Agostino McGowan, Romain François, Garrett Grolemond, et al. 2019. Welcome to the Tidyverse. *J. Open Source Software* 4 (43): 1686. 10.21105/joss.01686.

Further reading

- Andersson, L.R., Jesper, Stamatios Sotiropoulos. 2015. An integrated approach to correction for off-resonance effects and subject movement in diffusion MR imaging. *NeuroImage* 125 (October). 10.1016/j.neuroimage.2015.10.019.